Nuclear Engineering and Technology 51 (2019) 377–383

Contents lists available at ScienceDirect

Nuclear Engineering and Technology

journal homepage: www.elsevier.com/locate/net

Original Article

# Neutronic study of utilization of discrete thorium-uranium fuel pins in CANDU-6 reactor

Nianbiao Deng [a, b], Tao Yu [a, b, *], Jinsen Xie [a, b], Zhenping Chen [a, b], Qin Xie [a, b], Pengcheng Zhao [a, b], Zijing Liu [a, b], Wenjie Zeng [a, b]

[a] School of Nuclear Science and Technology, University of South China, Hengyang, Hunan, 421001, PR China
[b] Research Center for Digital Nuclear Reactor Engineering and Technology of Hunan Province, University of South China, Hengyang, Hunan, 421001, PR China

A R T I C L E I N F O

*Article history:*
Received 20 July 2018
Received in revised form
24 September 2018
Accepted 24 October 2018
Available online 25 October 2018

*Keywords:*
Th-U fuel
CANDU
Assembly schemes
Core schemes
Time-average model

A B S T R A C T

Targeting at simulating the application of thorium-uranium (TU) fuel in the CANDU-6 reactor, this paper analyzes the process using the code DRAGON/DONJON where the discrete TU fuel pins are applied in the CANDU-6 reactor under the time-average equilibrium refueling. The results show that the coolant void reactivity of the assembly analyzed in this paper is lower than that of 37-element bundle cell with natural uranium and 37-element bundle cell with mixed TU fuel pins; that the max time-average channel/bundle power of the core meets the limits - less than 6700kW/860 kW; that the fuel conversion ratio is higher than that of the CANDU-6 reactor with natural uranium; and that the exit burnup increases to 13400 MWd/tU. Thus, the simulation in this paper with the fuel in the 37-element bundle cell using discrete TU fuel pins can be considered to be applied in CANDU-6 reactor with adequate modifications of the core structure and operating modes.


## 1. Introduction

With the uranium mined in the last decades and a current nuclear power exceeding 393 GWe worldwide [1], accessible resources are easily becoming scarce.

The thorium-based fuel, as an option for advanced nuclear fuel system, offers potential advantages compared with traditional uranium-based fuel. Thorium fuel is more abundant-about three times-than uranium fuel reserves. Contrary to the $^{238}U$-$^{239}Pu$ fuel cycle where the breeding of fissile material can be obtained only with fast neutron spectra, the most superiority for thorium fuel cycle is that the $^{232}Th$-$^{233}U$ breeding cycle can operate with fast, epithermal or thermal spectra. The strong high energy gamma radiations emitted from the short lived daughter of $^{232}U$ enhance the non-proliferation of irradiated thorium based fuel. In thorium fuel cycle, much lesser quantities of transuranium element (TRU) are generated making long term radiotoxicity of waste decrease in a great deal. Thorium dioxide ($ThO_2$) has better thermo-physical properties because of its higher melting point, higher thermal conductivity and lower thermal expansion coefficient than that of uranium dioxide ($UO_2$) [2,3]. Therefore, utilization of thorium fuel is beneficial for the sustainable development of nuclear fission energy.

$^{232}Th$ conversion in $^{233}U$ is produced by neutrons provided by a fissile fuel, which should be as cheap as possible in an economical optimization context. For this purpose, SEU(slightly enriched uranium) is selected as the driver fuel. To minimize the costs of the reactor, in addition to minimizing fuel cost, choosing a system as flexible as possible and providing spare neutrons for thorium conversion are also essential.

The CANDU-6 reactor used by China's Third Qinshan nuclear power plant - a proven technology and commercial nuclear power plant - has been operating successfully for nearly 15 years. The CANDU-6 reactor has following features:

1) The CANDU-6 reactor which uses heavy water, as the moderator and the coolant, has high utilization of core neutrons and low requirements for backup reactivity. It makes thorium reactor can be driven by SEU.
2) A simple fuel bundle design provides convenient conditions for fuel composition optimization.

* Corresponding author. School of Nuclear Science and Technology, University of South China, Hengyang, Hunan, 421001, PR China.
*E-mail address:* yutao29@sina.com (T. Yu).

https://doi.org/10.1016/j.net.2018.10.022

3) The independent design of fuel channel makes it possible to carry out independent fuel management for the channel of different types of fuel in the same core.
4) On-power refueling is applied in CANDU-6 reactor, that makes reactivity of the core can be finely managed without a lot of residual reactivity, that reduces retention time of the strong neutron poison $^{232}$Th in the core, and that decreases the impact of $^{232}$Th on the core neutron economy.
5) Since the heavy water reactor has the softer neutron energy spectrum than the pressurized water reactor, the content of $^{232}$U is far lower than that of pressurized water reactor when the $^{232}$Th is used to produce $^{233}$U [4].

All these features of CANDU-6 reactor could be of great benefit in the implementation of thorium fuel cycle.

The CVR (coolant void reactivity) of the CANDU-6 reactor with NU (natural uranium) is positive [5], which is an unsafe factor. In addition, the CVR can be reduced by employing thorium fuel [6].

Currently, for the research of TU fuel application in CANDU-6 reactor, more are applied in mixed TU fuel pins [7–10]. On the other hand, CANDU-6 reactor applied to fuel pins with discrete TU is rarely studied.

Following previous correlative researches, the once-through scheme [11] is employed, to study the employment of 37-element bundle with discrete TU fuel pins (DTU-37) in CANDU-6 reactor in terms of the $^{235}$U enrichment and the arrangement of thorium pins. Comparing with the 37-element bundle cell using natural uranium (NU-37) and the 37-element bundle cell using the mixed TU fuel rods (MTU-37). The screened out thorium-based core scheme has higher fuel conversion ratio as well as smaller CVR and provides a reference for TU fuel in CANDU reactors.

First, the CANDU-6 reactor modeling methodology and fuel preliminary selection criteria is described in Section 2. Then Section 3 introduces the scheme devising of DTU-37. The lay out CANDU-6 reactor under the time-average equilibrium refueling is then presented in Section 4. Finally, conclusions are discussed in Section 5.

## 2. CANDU-6 reactor modeling and fuel selection

This research is based on the CANDU-6 reactor in Canada. The cylindrical reactor vessel contains 380 horizontal (Z-axis) fuel channels placed on a square lattice pitch of 28.575 cm. The coolant flows through two adjacent channels in opposite directions. A channel contains 12 identical fuel bundles 49.53 cm long. The usual 8-bundle shift refueling procedure is showed in Fig. 1.

The 37-element bundle is the assembly of CANDU-6 reactor [10], has 1, 6, 12 and 18 fuel pins per ring, which is illustrated in Fig. 2. In the 37-element bundle, each pin has the same diameter. The parameters of 37-element bundle cell for natural uranium is listed in Table 1 [12].

There are six types of reactivity control devices in a CANDU: 21 stainless steel adjuster rods (ADJ) normally insert in the core to provide a positive reactivity bank and to flatten the flux distribution; 14 liquid zone controllers (LZC) to manage the daily CANDU-6 reactor power control; 4 mechanical control absorbers (MCA)

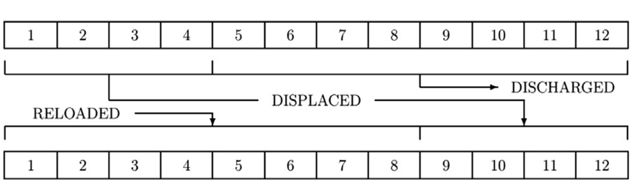


**Fig. 1.** 8-Bundle shift channel refueling procedure.

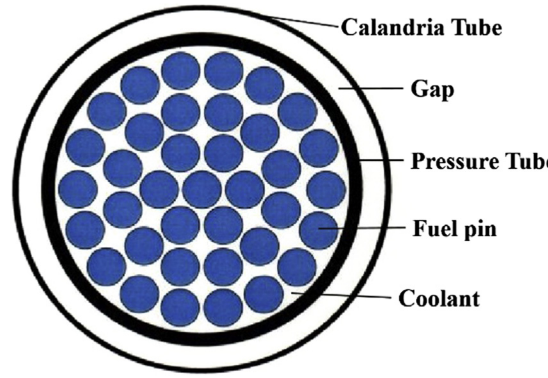


**Fig. 2.** Structure of 37-element bundle cell.

normally placed outside the core and inserted for bulk power control; 28 shutoff rods (SOR) suspended above the core and used for reactor shut down; boron poisoning nozzles (BPN) and gadolinium poisoning nozzles (GPN). Since all the reactivity devices are perpendicular to the fuel channels, accurate devices modeling should pass through 3D transport calculations, also called supercell calculations. Devices are located at lattice interstitial sites, as shown in Fig. 3 for a Y-oriented device. Here, BPN and GPN are not simulated [12].

### 2.1. Assembly modeling and fuel preliminary selection

For assembly modeling, firstly, transport calculations are performed with a nuclear data library on a 2D assembly model to generate 2-group condensed and assembly homogenized diffusion coefficients $D^G(B)$ with burnup ($B$) and macroscopic cross sections $\Sigma_x^G(B)$ for each reaction of type $x$. Another multigroup library is generated for use in the supercell models. 3D transport calculations are then performed for various devices to generate 2-group condensed and homogenized incremental macroscopic cross sections $\Delta\Sigma_x^G$ and diffusion coefficients $\Delta D^G$ libraries coherent with the 2D fuel properties [12]. The neutron transport code DRAGON [13] has various algorithms to deal with the 2D and 3D transport calculations [14]. Therefore, this open source code is well-suited for a numerical study of TU fuel cycles in CANDU-6 reactor.

For the calculation of 37-element bundle, the Wigner-Seitz approximation is employed, and the collision probability method (CP) for transport calculation. The generalized Stamm'ler method and Livolant-Jeanpierre resonance correction are used in resonance calculation. Assembly meshing: moderator is divided into 150 zones, each of the zirconium alloy pipe and insulated air gap for the 2 regions, the coolant is distinguished into 2 zones, the fuel pins are divided into 6 regions. The endfb7gx library of 172-group WIMSD-formatted library based on the ENDF/B-VII evaluated nuclear data library [15] is chosen, for the cross section library used in the DRAGON code.

Next, the performance metrics for selecting thorium-based fuels using simplified lattice calculations is described.

Negative reactivity feedback is beneficial to the inherent safety of the reactor, and CVR (in mk = 100pcm) is an important reactivity feedback for CANDU-6 reactor. The CVR stands for the total and instantaneous effect of loss of coolant on lattice reactivity:

$$\mathrm{CVR} \equiv \Delta\rho = \rho_{\mathrm{cooled}} - \rho_{\mathrm{viod}} = \frac{1}{k_{\mathrm{cooled}}} - \frac{1}{k_{\mathrm{void}}} \tag{1}$$

with the subscript “void” and “cooled” to indicate the zero and standard density of coolant, respectively.

**Table 1**
The parameters of NU-37.

| Structure | Material | Temperature(K) | Density (g/cm3) | Internal radius (mm) | External radius (mm) |
|---|---|---|---|---|---|
| Fuel | $UO_2$ | 941.3 | 10.44 | – | 6.12 |
| Cladding | Zr-II | 560.7 | 6.44 | 6.12 | 6.54 |
| Coolant | $D_2O$ | 560.7 | 0.81 | – | 51.69 |
| Pressure tube | Zr-Nb | 560.7 | 6.57 | 51.69 | 56.03 |
| Gap | $^4He$ | 345.7 | 0.0014 | 56.03 | 64.48 |
| Calandria tube | Zr-II | 345.7 | 6.44 | 64.48 | 65.87 |
| Moderator | $D_2O$ | 345.7 | 1.08 | 65.87 | – |

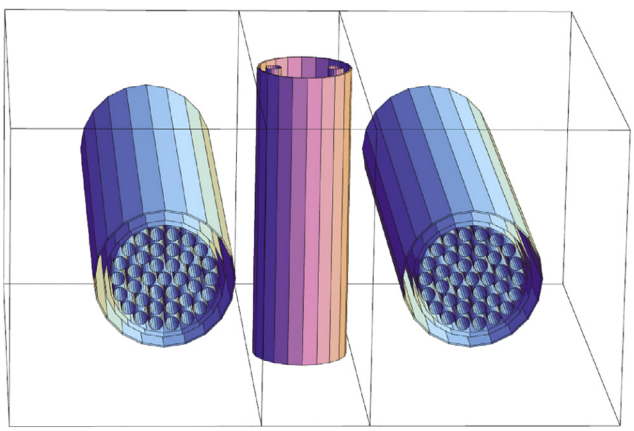

**Fig. 3.** Fuel channels reactivity device.

The assembly of CANDU-6 reactor has a positive CVR [5] because of the pitch of lattice is large and stays in the overmoderated area. Moreover, with the use of thorium fuel, by optimizing design, the assembly's CVR can be decreased and its intrinsic safety enhanced.

For the sake of evaluating the conversion ability of fuels, the concept of fissile inventory ratio (FIR) is introduced [16]:

$$FIR(t) = \frac{N_{fissile}(t)}{N_{fissile}(0)} \quad (2)$$

Where $N_{fissile}(t)$ represents the atomic density of fissile nuclides at a given moment, and $N_{fissile}(0)$ represents the atomic density of fissile nuclides at the initial time. For uranium-thorium cycles, $^{233}Pa$ and $^{239}Np$ decay to $^{233}U$ and $^{239}U$ after the fuel has been discharged, consequently, they are treated as fissile nuclides in FIR calculate.

### 2.2. Reactor core modeling and fuel preliminary selection

For core modeling, firstly, to calculate the cross-section with reflector.

At the most probable core burnup, a reactor database containing the reflector is created, then perform a supercell calculation to produce incremental cross sections $\Delta\Sigma_x^G$ (and diffusion coefficients $\Delta D^G$), which reflect the effect of the reflector on the average cross section of the assembly.

The full-core diffusion model is established by taking the cross-section of the reflector introduced above and the assembly's macroscopic cross sections of burnup-dependent fuels as well as reactivity devices in Section 2.1. The neutron diffusion code DONJON [17] deals with the 2-group diffusion equation for the finite core. This code has a variety of algorithms to handle on-power fuel management [18]. Thus, this open-source code is suitable for a numerical study of TU fuel cycles in CANDU-6 reactor. The grid size of core is set to 10 cm.

The reliability of the results on CANDU-6 reactor with TU fuel obtained from DRAGON/DONJON code system, has been verified by dozens of studies before [7–10,19].

Then, to introduce several principles are considered when screening out thorium-based fuels in the optimization design of core:

1) The $k_{eff}$ in the equilibrium period should be similar to the $k_{eff}$ in the actual equilibrium period in the CANDU-6 reactor. The minimum excess reactivity of the CANDU-6 reactor is 1.5 mk [20]. Taking into account the range of reactivity control of the LZC is smaller, the $k_{eff}$ design interval of the core requires 1.0015–1.0025.
2) The refueling rate of core schemes should be less than that of the CANDU-6 reactor with NU-37.
3) The maximum time-average channel power should be less than 6700 kW, the maximum time-average bundle power should be less than 860 kW.
4) Only consider the adjuster rods and the LZC for the reactivity devices. The adjuster rods are all inserting into the core. The liquid level of the LZC is fully setting to 50% [10].

The normalized uranium contents

$$NUC = \frac{e_U V_U}{e_{nat_U} V_{nat_U}} \quad (3)$$

is introduced to compare the fissile nuclide contents of different configurations and fuels.

And $e_u$ is the initial uranium enrichment in $UO_2$, Vu denotes in the initial phase, and the uranium fuel accounts for the volume of the entire bundle of fuel. $^{nat}U$ means natural uranium ($V^{nat}_U$ is 100%).

In order to evaluate the conversion ability of the fuel in the whole cycle, $\Xi$ - the ratio of the average discharge burnup for the given core $B^e$ to the reference core average exit burnup $B^e_{ref}$ - is introduced:

$$\Xi = \frac{B^e}{B^e_{ref}} \quad (4)$$

It indicates that how much energy can be extracted from the initial fission nuclide in a given cycle compared to the NU cycle [10].

## 3. The scheme design of DTU-37

For the layout of DTU-37, all the arrangements of the thorium pins placed 1, 2, 3, 4 rings (thorium rods placed on 1st ring, 2nd ring, …, 2nd, 3rd,4th ring, a total of 14 species, regardless of the full use of thorium pins)is considered. The uranium rod with a SEU fuel, $^{235}U$ enrichment options for 1%, 1.5%, 2%, 2.5%. Based on the arrangement of thorium pins and enrichment of SEU, a total of 56 assembly cases are obtained. The densities of $UO_2$ and $ThO_2$ are 10.44 g/cm$^3$ and 10.0 g/cm$^3$, respectively.

The DRAGON code is employed to calculate the assembly parameters. By adjusting the enrichment of uranium pins and the arrangement of thorium pins, the design of the assembly is carried out from the aspects of reactivity coefficient and fuel conversion ratio.

### 3.1. CVR-based assembly design

The physical parameters of 56 kinds of DTU-37 cases under zero burnup is calculated, and select schemes with negative CVR as well as $k_{inf}$ is greater than 1 (Table 2).

Fig. 4 shows the CVR respecting to burnup for the 3 kinds of DTU-37 cases listed in Table 2, taking into account restart condition, compared to the corresponding MTU-37 and NU-37. The burnup calculation for the assembly is completed when $k_{inf}$ is decreased to 1.040 [21]. The CVR of the DTU-37 schemes selected in Table 2 are much less than that of MTU-37 and NU-37 over the lifetime of the assembly, and are substantially all negative. Only the CVR of case 3 becoming positive when the last lifetime. The $k_{inf}$ of corresponding MTU-37 cases of case 1 and case 2 are less than 1.040 at zero burnup, and those CVR are 16.4mk and 17.7mk, respectively, which are much larger than the corresponding DTU-37 cases. It can be seen that the DTU-37 schemes screened in Table 2 have better intrinsic safety.

### 3.2. Quantitative analysis the CVR of TU fuel assembly by MCNP

In order to quantitatively analyze the CVR of DTU-37 and corresponding MTU-37, the MCNP code is used to calculate the nuclear reaction rate at zero burnup condition.

The energy groups are divided according to the cross-section library of WMIS 69-group and ignore the change of the average fission neutron number $\nu$, then

$$k_{inf}=\frac{\sum_{g=1}^{69} vR_f}{\sum_{g=1}^{69} R_a} \tag{5}$$

According to (5), CVR can be formulated as:

$$\mathrm{CVR} = (\mathrm{kvoid} - \mathrm{kcooled})/\,\mathrm{kvoid}\cdot \mathrm{kcooled} = \frac{\left(\frac{\sum_{g=1}^{69} vR_f}{\sum_{g=1}^{69} R_a}\right)_{void} - \left(\frac{\sum_{g=1}^{69} vR_f}{\sum_{g=1}^{69} R_a}\right)_{cooled}}{\left(\frac{\sum_{g=1}^{69} vR_f}{\sum_{g=1}^{69} R_a}\right)_{void} \times \left(\frac{\sum_{g=1}^{69} vR_f}{\sum_{g=1}^{69} R_a}\right)_{cooled}} \tag{6}$$

Case 3 compares with its corresponding MTU-37 for nuclear reaction rate (Table 3). Table 3 indicates, in terms of DTU-37, after LOCA occurs, the fission reaction rate is reduced by 2.12E+15, the absorption reaction rate is reduced by 1.90E+15, it can be concluded from above that, the former is reduced more, the increases of neutron is less than the decreases, thus, CVR is negative. For the MTU-37, after LOCA occurs, the fission reaction rate is reduced by 1.82E+15, the absorption reaction rate is reduced by 2.63E+15, the former is reduced less, so the CVR positive.

From the above calculations show that MCNP program is used to quantitatively calculate the nuclear reaction rate of TU fuel assemblies. From the perspective of Monte Carlo method, we can preliminarily verify the CVR of DTU-37 is smaller than that of MTU-37.

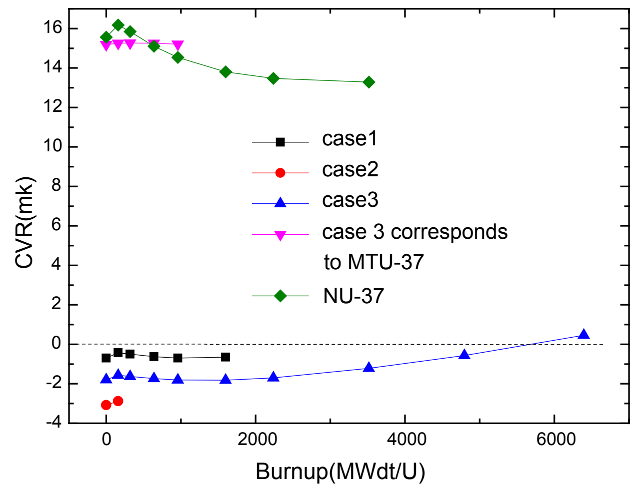


**Fig. 4.** The CVR of different assembly schemes change with burnup.

**Table 3**
The nuclear reaction rate of Case 3 as well as its corresponding MTU-37 before and after the occurrence of LOCA.

| | Case 3 | | Case 3 corresponding MTU-37 | |
|---|---|---|---|---|
| | Cooled | Void | Cooled | Void |
| $\sum_{g=1}^{69} R_f$ | 2.323E+16 | 2.111E+16 | 2.245E+16 | 2.063E+16 |
| $\sum_{g=1}^{69} R_a$ | 2.310E+16 | 2.120E+16 | 2.501E+16 | 2.238E+16 |
| $\frac{\sum_{g=1}^{69} R_f}{\sum_{g=1}^{69} R_a}$ | 1.01E+00 | 9.96E-01 | 8.98E-01 | 9.22E-01 |
| CVR | −9.86E-03 (1/ν) | | 2.92E-02 (1/ν) | |

### 3.3. FIR-based assembly design

Fig. 5 gives the FIR respecting to burnup for the 3 kinds of DTU-37 schemes listed in Table 2, compared to the NU-37 and MTU-37. The burnup calculation for the assembly is completed when $k_{inf}$ is decreased to 1.040. It shows that under the same TU fuel composition conditions, the DTU-37 cases selected in Table 2, can get deeper burnup depth, which means higher utilization of neutrons. The FIR value of DTU-37 is close to that of MTU-37, which is larger than that of the NU-37, thus, DTU-37 has better fuel conversion ratio.

In the core of DTU-37 under our consideration, fission neutrons are mainly generated by the uranium rod in the outermost ring of the assembly and are sufficiently moderated in the heavy water between the assembly and the assembly, where it is absorbed to induce new fission. The pitch of pins is small, which makes the fully

**Table 2**
DTU-37 cases with negative CVR and $k_{inf}$ is greater than 1.

| Cases | Arrangement of thorium pins | Enrichments of $^{235}U$ (%) | $k_{inf}$-cooled | $k_{inf}$-void | CVR (mk) |
|---|---|---|---|---|---|
| Case1 | on 2nd, 3rd ring | 2.0 | 1.1154 | 1.1145 | **−0.691** |
| Case 2 | on1st, 2nd, 3rd ring | 2.0 | 1.0895 | 1.0858 | **−3.084** |
| Case 3 | on1st, 2nd, 3rd ring | 2.5 | 1.1812 | 1.1787 | **−1.793** |

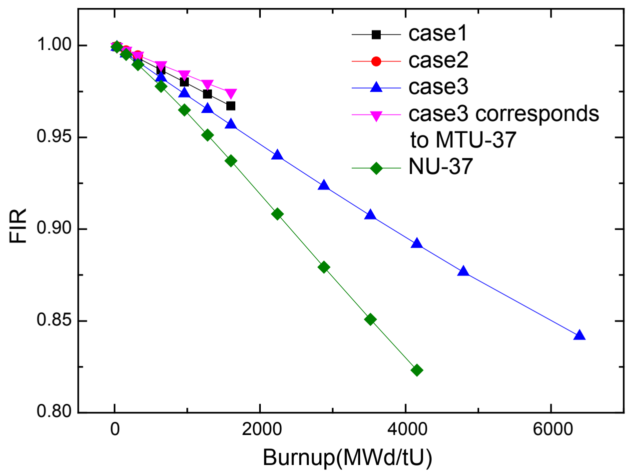


**Fig. 5.** The FIR of different assembly schemes change with burnup.

moderated neutrons are mostly absorbed by the outermost uranium pins in the core of DTU-37, while the neutrons absorbed by the inner rings of thorium pins relatively decreases. That is, outer uranium rods produced a "space shield" effect on the inner thorium rods, which makes FIR is lower for DTU-37 than for those MTU-37 and slightly reduces fuel conversion ratio.

To sum up, in the premise of ensuring more reliable safety, the 3 groups of the DTU-37 cases selected in Table 2 have also larger fuel conversion ratio than NU-37. Thus, these 3 assemblies are used as the alternative assembly cases to the core scheme design.

## 4. The optimization design of core scheme in CANDU-6 reactor under the time-average equilibrium refueling

The DONJON program is used to calculate the time-average diffusion of the reactor core. The radial core refueling strategy and the axial refueling strategy are adjusted to select the core optimization schemes that meets safety criteria and high fuel conversion ratio, and compared with the CANDU-6 reactor using NU-37.

### *4.1. Introduction to fuel management in CANDU-6 reactor and time-average model*

#### *4.1.1. Fuel management in CANDU-6 reactor*

The design phase of fuel management in CANDU-6 reactor includes obtaining an ideal time-average power distribution, under the equilibrium core, which will be employed by the refueling engineer as the target power distribution during operation. On-power refueling features of CANDU-6 reactor has brought a great deal of flexibility for the target exit burnup and the axial refueling schemes of each region (or channel), which will greatly contribute to the design of time-average power/neutron flux shape [22]. The design phase of the fuel management is the main content of this study.

The fuel management strategy is divided into two components - the axial refueling strategy and the radial refueling strategy. For radial strategy, which is related to the channels refueling rate and is expressed in terms of the time-average channel exit burnup; for the other, the 8-bundle-shift refueling and 4-bundle-shift refueling are considered currently [10].

#### *4.1.2. Time-average model*

In the time-average model, the only time-average flux/power distribution over the entire core is obtained by averaging the neutron flux and power at each fuel bundle over a substantial period of time. This shape can be used to calculate the parameters such as exit burnup and refueling frequency, and as the reference. The main task of fuel management in the design phase is to establish such distribution [22].

The time-average model has two free variables that need to be adjusted manually by the user based on theoretical knowledge and experience. One is the basic refueling scheme, several new fuel bundles are replaced each time the fuel channel is refuelled; the other is the target exit burnup of each fuel channel. The mathematical model discussed below will take a specific 8-bundle-refueling scheme as an instance.

For each fuel bundle position of the core, $B_{in}$ and $B_{out}$ are the values of fuel burnup when the fuel enters and exits that position in core, respectively, let $\varphi_{jk}$ be the time-average fuel flux at axial position k in channel j, k ranging from 1 to 12 (since there are 12 bundles per channel) and j ranging over the channels, e.g. from 1 to 380 in the CANDU-6 reactor. And $T_j$ is the dwell time of channel j (the average time interval between refuellings of channel j):

$$B_{out,jk}=B_{in,jk}+\varphi_{jk}\cdot T_j \tag{7}$$

Time-average nuclear cross sections are defined at each bundle position in the core by averaging the lattice cross sections over the burnup range [$B_{in}$, $B_{out}$] over time by fuel at the jk position.

$$\sum_{i,jk}^{Tavg}=\frac{\int_{B_{in,jk}}^{B_{out,jk}}\sum_i(B)dB}{B_{out,jk}-B_{in,jk}} \tag{8}$$

When a channel is refuelled with an 8-bundle-shift, the first 8 positions in the channel receive fresh fuel and the entrance irradiations for positions 9–12 are simply the exit burnup from positions 1 to 4 respectively, thus

$$B_{in,jk}=0 \quad k=1,\ldots,8 \tag{9}$$

$$B_{in,jk}=B_{out,j(k\text{-}8)},\ k=9,\ldots,12 \tag{10}$$

In addition to the refueling scheme, the time-average model has other degrees of freedom. These are the values of exit irradiation $B_{exit,\ j}$ for the different channels j. In principle there are as many degrees of freedom as there are channels. (Of course the values of exit burnup are not completely free, but are constrained by the requirement to maintain a critical reactor). The exit burnups are related to the flux in the following way. Taking the 8-bundle-shift refueling scheme as an example, bundles 5 to 12 leave the core at each refueling, then the exit burnup can be expressed as:

$$B_{exit,\ j}=\frac{1}{8}\sum_{k=5}^{12}B_{out,jk} \tag{11}$$

By equations (5), (7) and (8), where $B_{exit,j}$ is given by

$$B_{exit,\ j}=\frac{T_j}{8}\sum_{k=1}^{12}\Phi_{j,k} \tag{12}$$

Therefore, the dwell time $T_j$ is satisfied

$$T_j=\frac{8B_{exit,j}}{\sum_{k=1}^{12}\Phi_{j,k}} \tag{13}$$

All the equations required to calculate the time-average neutron flux shape are obtained. These equations are:

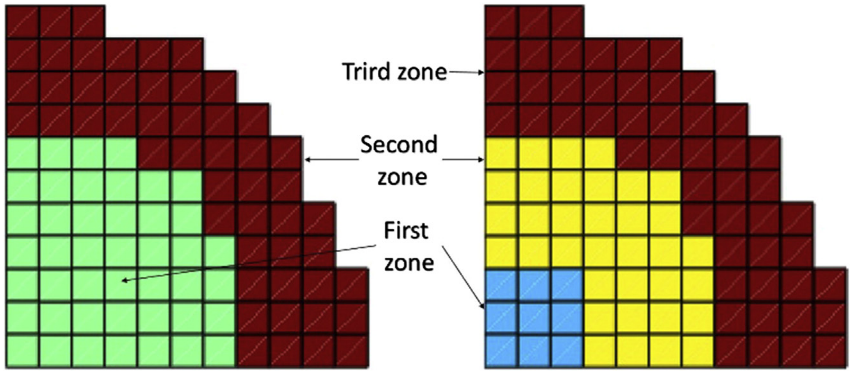


**Fig. 6.** Burnup partitions in radial.

**Table 4**
Verification of each assembly scheme of refueling frequency.

| Cases | Parameters | Values |
|---|---|---|
| NU-37 | Average exit burnup of each zone of core (MWd/$T_{he}$) | 8100/6400[a] |
| | $F$ (kg d$^{-1}$) | 0.7571 |
| Case 1 | Average exit burnup of each zone of core (MWd/$T_{he}$) | 4200/3800 |
| | $F$ (kg d$^{-1}$) | 1.3531 |
| Case 2 | Average exit burnup of each zone of core (MWd/$T_{he}$) | 550/450 |
| | $F$ (kg d$^{-1}$) | ∞ |
| Case 3 | Average exit burnup of each zone of core (MWd/$T_{he}$) | 14000/12700 |
| | $F$ (kg d$^{-1}$) | 0.4064 |

[a] 8100/6400, means zone 1, zone 2 average exit burnup value are 8100,6400 MWd/The, respectively, and so forth, the same below.

1) The time-independent finite difference neutron diffusion equation to solve the neutron flux distribution.
2) Equation (13) to calculate the residence time $T_j$ for each channel.
3) Equations (7), (9) and (10) are used to compute $B_{in,\ jk}$ and $B_{out,\ jk}$ for each fuel bundle in core.
4) Equation (8) (and similar equations for other cross sections) to calculate the time-average lattice parameters.

To solve this system of equations, the user needs to give the exit burnup of each fuel channel $B_{exit,\ j}$. For the sake of obtaining the desired neutron flux shape while taking into account the local neutron absorption caused by presence of extra "hardware" (device locators, etc., mostly at the bottom of the calandria), the DONJON program's time-average model generally divides the core into multiple burnup regions.

Since consistency must be achieved between the flux, the channel residence times, the individual-bundle burnup ranges [$B_{in}$, $B_{out}$] and the lattice properties, an iterative scheme between the solution of the diffusion equation and the other equations is employed until all quantities converge.

In general, users are required to iteratively determine the exit burnup $B_{exit,\ j}$ for each zone to obtain a critical reactor and a desired flux distribution [23].

### 4.2. The optimization design of core scheme

Based on the time-average model, we obtain better flux distribution, power distribution and burnup distribution by reasonably controlling the exit burnup of each zone in CANDU-6 reactor [22]. The reactor core will be divided into 2 zones and 3 zones, as shown in Fig. 6 [24]. Axial refueling strategy is considering 2 schemes - 8-bundle-shift refueling and 4-bundle-shift refueling.

Firstly, the refueling frequency needs to be analyzed. The core, distinguished into 3 burnup zones, employs the 8-bundle-shift refueling scheme, through the reasonable adjustment of exit burnup of each region (see Table 4), making the core $k_{eff}$ satisfy the specified range, the channel average refueling frequency $F$ for screening out the core scheme is less than that of using NU-37. From Table 4, only using the core scheme of case 3 meets the requirement that the frequency of refueling is less than that of CANDU-6 reactor with NU,therefore, case 3 is selected as the final assembly case.

Then, the assembly employs the case 3. The core, divided into 2 and 3 zones, is used for two kinds of axial refueling schemes:the 8-bundle-shift refueling as well as 4-bundle-shift refueling. By reasonably controlling the exit burnup of each region of the core, core schemes meeting all the principles are given and compared with the core schemes using NU. The results are shown in Table 5.

**Table 5**
Comparison of TU fuel with NU results of time-average calculations which meet all limits.

| Cases | Parameters | Values | | | |
|---|---|---|---|---|---|
| | | 8-bundle-shift refueling | | 4-bundle-shift refueling | |
| NU-37 | Exit burnup of each zone of the core/(MWd/tU) | 8000/6500 | 8200/7800/6650 | 7800/6900 | 8100/7700/7000 |
| | Core average exit burnup/(MWd/tU) | 7192.1 | 7231.5 | 7349.2 | 7390.9 |
| | Maximum time-average channel power/(kW) | 6665.8 | 6699.7 | 6613.1 | 6652.6 |
| | Maximum time-average bundle power/(kW) | 858.1 | 852.9 | 857.7 | 857.4 |
| | $F$/(kg day$^{-1}$) | 0.7542 | 0.7501 | 0.7381 | 0.7340 |
| Case 3 | Exit burnup of each zone of the core/(MWd/tU) | 14100/12700 (CaseIII-8-2)* | 13600/14100/12800 (CaseIII-8-3) | 14000/12100 (CaseIII-4-2) | 13500/13800/12450 (CaseIII-4-3) |
| | Core average exit burnup/(MWd/tU) | 13392.3 | 13404.2 | 13011.1 | 13103.0 |
| | Maximum time-average channel power/(kW) | 6621.6 | 6584.4 | 6562.7 | 6564.0 |
| | Maximum time-average bundle power/(kW) | 848.7 | 839.5 | 799.2 | 775.4 |
| | $F$/(kg day$^{-1}$) | 0.4051 | 0.4047 | 0.4169 | 0.4140 |

* CaseIII-8-2 means the core scheme with case 3 assembly,8-bundle-shift refueling and 2 districts, and so forth.

From Table 5, for core average exit burnup, the maximum exit burnup of the core scheme with case 3 can reach 13400 MWd/t(U), which is 80% higher than the 7300 MWd/t(U) with NU; for the frequency of refueling, the use of case 3 is about 0.41, compared with the use of NU reached 0.73 reduced by more than 80%; and for maximum time-average channel/bundle power, the use of case 3 are smaller than the use of NU. Therefore, the core schemes with the case 3 can significantly reduce the refueling frequency and greatly improve the core exit burnup, under the premise of being able to have a smaller maximum time-average channel/bundle power.

For the four kinds of core schemes of Table 5 using the case 3, the 8-bundle-shift refueling schemes have a larger core exit burnup, a smaller refueling frequency, and a slightly larger maximum channel/bundle power than the 4-bundle-shift refueling schemes'. For the core divided into two regions and three regions, both exit burnup in the schemes are similar. The core divided into three zones can obtain smaller maximum time-average channel/bundle power, effectively control the local power, and make the reactor obtain sufficient operating margin. Thus, the case III-8-3, which has lower maximum time-average channel/bundle power and maximum exit burnup.

Taking case III-8-3 as given scheme, the reference scheme for the maximum scheme of exit burnup in NU schemes, the calculation gives $\Xi/NUC = 1.0608$, which is greater than 1, indicating the fuel conversion ratio using scheme III-8-3 is higher than the CANDU-6 reactor with NU.

Based on the above analysis, the case III-8-3 can have higher fuel conversion ratio, minimum refueling frequency and maximum reactor exit burnup, under the premise of ensuring effective control of local power and achieving sufficient operation margin of the reactor, which is the recommended core optimization scheme.

## 5. Conclusions

Based on the existing TU fuel cycle in CANDU-6 reactor, the assembly, using 37-element bundle with discrete TU fuel pins, is studied from aspects of enrichment of uranium fuel and arrangement of thorium rods. The core is conducted time-average study form aspects of fuel burnup zone, the district of exit burnup and other.

The results show that the CANDU-6 reactor with adequate modification of the structure of the core as well as operation modes, the assembly using 37-element bundle with discrete TU fuel pins consists of 2.5 wt% $UO_2$ and thorium pins which are placed on its first, second and third rings; the core, distinguished into 3 burnup zones, employs the 8-bundle-shift refueling scheme. It meets the time-average channel/bundle constraint, provides lower coolant void reactivity than NU as well as MTU-37 and higher fuel conversion ratio than that of the CANDU-6 reactor with NU, and the exit burnup increased to 13400 MWd/tU. Our simulation preliminarily verifies the feasibility application of discrete TU fuel pins in CANDU-6 reactor, which provides a reference for TU fuel in CANDU reactors.

## Acknowledgments

This work is supported by the National Natural Science Foundation of China (Nos. 11575079, 11605085) and 2018 Graduate Research and Innovation Project of Hunan Province, PR China (Preliminary study on physical properties of utilization of discrete thorium-uranium fuel assembly in CANDU-6 reactor). The authors would like to show their great appreciations to NEAL (Nuclear Engineering and Application Laboratory) Team for its contribution to this research.

## Appendix A. Supplementary data

Supplementary data to this article can be found online at https://doi.org/10.1016/j.net.2018.10.022.

## References

[1] IAEA, Power Reactor Information System, 2017. http://www.iaea.org/pris/.
[2] G. Zhang, T. Yu, J.S. Xie, et al., Validation of thorium fuel benchmark by DRAGON code using WLUP library, Atomic Energy Sci. Technol. 50 (10) (2016) 1828–1833 (in chinese).
[3] International Atomic Energy Agency, Thorium Fuel Cycle: Potential Benefits and Challenges, IAEA-tecdoc-1450, 2005 (Vienna, Austria).
[4] Z.H. Zhang, M.J. Chen, Technical advantage of HWR and the tentative plan for its development, China Nuclear Power 03 (02) (2010) 124–129 (in chinese).
[5] J.Q. Qian, Characteristics and development of CANDU NPP unit, Chinese J. Nucl. Sci. Eng. 23 (03) (2003), 193-20 2+210 (in chinese).
[6] Y.H. Wang, K. Wang, Research on physics characteristics of the fuel for thorium-based heavy water nuclear energy system, Nucl. Power Eng. 24 (05) (2003) 454–457 (in chinese).
[7] A. Nuttin, P. Guillemin, T. Courau, et al., Study of CANDU thorium-based fuel cycles by deterministic and Monte Carlo methods, in: PHYSOR 2006, Vancouver, Canada, 2006.
[8] T.L. Wang, J.H. Li, Research on U-Th self-sustaining cycle in CANDU, Chinese J. Nucl. Sci. Eng. 30 (02) (2010) 144–149 (in chinese).
[9] B. Holmes, Automated Refueling Simulations of a CANDU for the Exploitation of Thorium Fuels (Ph.D. thesis), École Polytechnique de Montréal, Montréal, Canada, 2013.
[10] E. St-Aubin, CANDU-6 fuel optimization for advanced cycles, Nucl. Eng. Des. 293 (2015) 371–384.
[11] M.S. MILGRAM, Once through Thorium Cycles in CANDU Reactors, Atomic Energy of Canada Report, AECL-7516, 1982.
[12] E. St-Aubin, G. Marleau, Optimized CANDU-6 cell and reactivity device supercell models for advanced fuels reactor database generation, Ann. Nucl. Energy 85 (2015) 331–336.
[13] G. Marleau, A. Hebert, R. Roy, A User Guide for DRAGON Version4, Report IGE-294, École Polytechnique de Montréal, Montréal, Canada, 2016.
[14] G. Marleau, New Geometries Processing in DRAGON: the NXT: Module, Report IGE-260 Rev.1, École Polytechnique de Montréal, Montréal, Canada, 2006.
[15] WLUP, Final stage of the WIMS-D library update project. http://www-nds.iaea.org/wimsd, 2014.
[16] S.C. Liu, J.J. Cai, Neutronics study of uranium-thorium mixed fuel assembly in SCWR, Nucl. Sci. Eng. 35 (03) (2015) 6–7 (in chinese).
[17] A. Hebert, D. Sekki, R. Chambon, A User Guide for DONJON Version4, Report IGE-300, École Polytechnique de Montréal, Montréal, Canada, 2016.
[18] R. Chambon, E. Varin, D. Rozon, CANDU fuel management optimization using alternative gradient methods, Ann. Nucl. Energy 34 (2007) 1002–1013.
[19] A. Nuttin, P. Guillemin, A. Bidaud, et al., Comparative analysis of high conversion achievable in thorium-fueled slightly modified CANDU and PWR reactors, Ann. Nucl. Energy 40 (2012) 171–189.
[20] W.C. Wang, J.J. Feng, J. Wang, et al., Development of software system for optimization of CANDU refueling, China Nucl. Ind. (11) (2011) 11–17 (in chinese).
[21] S.F. Shen, Y.G. Wang, K. Wang, et al., Research on fuel cycle of thorium advanced CANDU reactor, Atomic Energy Sci. Technol. 41 (02) (2007) 194–198 (in chinese).
[22] S.H. Zhang, J.Q. Shan, Fuel management of CANDU reactor, Nucl. Power Eng. 20 (6) (1999) 543–548 (in chinese).
[23] B. Rouben, Fuel Management in CANDU, Report, AECL, 1997, pp. 11–14.
[24] R. Chambon, Optimisation de la gestion du combustible dans les réacteurs CANDU refroidis à l'eau légère (Ph.D. thesis), École Polytechnique de Montréal, Montréal, Canada, 2006.